Naval Research Laboratory
Washington, DC 20375-5320

NRL/MR/6790--97-7885

Active Remote Sensing Using Ultra Broadband Radiation

P. SPRANGLE
A. TING
E. ESAREY
R. HUBBARD

Beam Physics Branch
Plasma Physics Division

B. HAFIZI

ICARUS Research Inc.
Bethesda, MD

January 31, 1997

REPORT DOCUMENTATION PAGE

Form Approved
OMB No. 0704-0188

1. AGENCY USE ONLY *(Leave Blank)*	2. REPORT DATE	3. REPORT TYPE AND DATES COVERED
	January 31, 1997	Interim Report

4. TITLE AND SUBTITLE

Active Remote Sensing Using Ultra Broadband Radiation

5. FUNDING NUMBERS

6. AUTHOR(S)

P. Sprangle, A. Ting, E. Esarey, R. Hubbard, and B. Hafizi*

7. PERFORMING ORGANIZATION NAME(S) AND ADDRESS(ES)

Naval Research Laboratory
Washington, DC 20375-5320

8. PERFORMING ORGANIZATION REPORT NUMBER

NRL/MR/6790--97-7885

9. SPONSORING/MONITORING AGENCY NAME(S) AND ADDRESS(ES)

Office of Naval Research
Arlington, VA 22217-5660

10. SPONSORING/MONITORING AGENCY REPORT NUMBER

11. SUPPLEMENTARY NOTES

*ICARUS Research, Inc.
P.O. Box 30780
Bethesda, MD 20824-0780

12a. DISTRIBUTION/AVAILABILITY STATEMENT

Approved for public release; distribution unlimited.

12b. DISTRIBUTION CODE

13. ABSTRACT *(Maximum 200 words)*

Active remote sensing using ultra broadband (UB) radiation has the potential to achieve identification of hazardous air pollutants (HAPs) at extended distances. The objective of this report is to propose and analyze the use of UB radiation for active remote sensing of HAPs. The UB source can provide day-night illumination of the pollution site with simultaneous multi-wavelength (continuum) radiation in the ultraviolet, visible or infrared regime. In addition, the UB radiation can be used in a multi-wavelength DIAL (DIfferential Absorption Lidar) configuration. One unique feature of this approach is the high average power achieved by using two long duration lasers at slightly different frequencies beating in a nonlinear medium. In addition, a demonstration experiment on the generation of UB radiation by this method is described.

14. SUBJECT TERMS

Remote sensing
Ultra broadband radiation
Hazardous air pollutants
Supercontinuum generation
Lidar
Dial

15. NUMBER OF PAGES

30

16. PRICE CODE

17. SECURITY CLASSIFICATION OF REPORT	18. SECURITY CLASSIFICATION OF THIS PAGE	19. SECURITY CLASSIFICATION OF ABSTRACT	20. LIMITATION OF ABSTRACT
UNCLASSIFIED	UNCLASSIFIED	UNCLASSIFIED	UL

CONTENTS

ACTIVE REMOTE SENSING USING ULTRA BROADBAND RADIATION

I. Introduction

The possibility of detecting the constituents of the atmosphere and measuring atmospheric properties was proposed soon after the invention of the laser. LIDAR (LIght Detection and Ranging) technology encompasses a number of techniques for remote sensing of the atmosphere. The fundamental physical processes involved in lidar include: i) Rayleigh scattering, ii) Mie scattering, iii) Raman scattering, iv) resonant absorption, v) resonant scattering, and vi) fluorescence.[1] These physical processes form the basis of lidar techniques that can be used in varied environments. Lidar techniques include: i) atmospheric backscatter lidar, ii) resonance scattering lidar, iii) DIfferential Absorption Lidar (DIAL), iv) fluorescence lidar, v) Raman lidar, and vi) Doppler lidar.

A key element of lidar is the radiation source. Source characteristics tend to be critical in lidar measurements since they dictate the interaction physics, the received signal and ultimately the signal to noise ratio. Relevant source characteristics include: i) spectral profile, ii) spectral brightness, iii) pulse energy, iv) pulse shape, v) pulse duration, vi) pulse repetition rate, vii) beam divergence, viii) polarization, and ix) coherence properties.

Active remote sensing has been pursued almost exclusively with lasers of various kinds. Lasers are highly effective in many respects since they can be extremely bright and highly directed. In many applications, however, the narrow spectral bandwidth of conventional lasers limits their utility. For example, in DIAL it is necessary to have the capability to scan across the absorption spectrum of the molecular species. In many cases the gain bandwidth of the available source is either not close enough to the molecular transition or not sufficiently broad to encompass the

Manuscript approved December 16, 1996

absorption spectrum. It is desirable, therefore, to have a source that shares with lasers such useful characteristics as brightness and directionality and yet is sufficiently broadband to permit target identification over a wide spectral range.

The objective of this report is to discuss the remote sensing capability of ultra broadband (UB) sources of radiation [2] that are capable of detecting and monitoring multi species hazardous air pollutants (HAPs). Current monitoring techniques are not capable of detecting many of the HAPs in real time or on a continuous basis. In conventional remote sensing, the received signal from the pollutant is usually from the scattering of sunlight or a single, tunable laser line. The relatively narrow tuning ranges of lasers and the inability of these lasers for fast, real-time tuning restrict the use of LIDAR and DIAL to the detection and ranging of a select group of predetermined pollutants.

A schematic of a UB remote sensing configuration is shown in Fig. 1. A modulated laser interacting with a nonlinear medium generates UB radiation which is reflected from a parabolic mirror and propagated over extended distances to the region of the HAPs. The scattered radiation having the spectral signatures of the HAPs is received and analyzed. The unique features of this approach are the high average power possible with the laser beat wave UB source and the capability of simultaneously interrogating multiple HAPs.

The advent of ultrashort laser technology has ushered a new era of time-resolved spectroscopy, with pulses so short that one can now study nonequilibrium states of matter, and explore new frontiers in science and technology. One of the most important nonlinear optical processes with ultrashort pulses is supercontinuum generation - the production of intense ultrashort broadband "white light" pulses.[2,3]

The first study of the mechanism and generation of ultrashort supercontinuum dates back to 1969, when Alfano and Shapiro observed the first "white" picosecond pulse continuum in liquids and solids.[2,4] The observed spectra extended over ~ 6000 cm^{-1} in the visible and infrared wavelength region. The large spectral broadening of ultrashort pulses was attributed to self-phase modulation (SPM) arising from anharmonic electronic oscillations and a model of supercontinuum generation was formulated. Over the years, advances in mode-locked lasers have led to the production of wider super-continua in the visible, ultraviolet, and infrared wavelength regions using various materials.

The supercontinuum arises from the propagation of intense picosecond or shorter laser pulses through condensed or gaseous media. When an intense laser pulse propagates through a medium, it changes the refractive index, which in turn changes the phase, amplitude, and frequency of the pulse. Supercontinuum laser sources can be wavelength selected and coded simultaneously over wide spectral ranges (up to 10,000 cm^{-1}) in the ultraviolet, visible, and infrared regions at high repetition rates, gigawatt output peak powers, and femtosecond pulse durations. Ultrashort supercontinuum pulses have been used for time-resolved absorption spectroscopy and material characterization. The applications of interest here include spectroscopy, three-dimensional imaging, and ranging in atmospheric remote sensing.

The plan of this report is as follows. In Section II we discuss the generation of UB radiation. Section III presents results of numerical studies of UB radiation generation. In Section IV we show that with the use of three wavelengths a significant improvement in the usual (two-wavelength) DIAL method is possible. In particular, it is shown that knowledge of the dependence of the reflectivity and extinction coefficient on wavelength is not necessary if three or

more wavelengths are used. Section V presents a discussion of an experiment where UB radiation is generated in the near IR, with application to the detection of HAPs. Section VI summarizes the report.

II. Ultra Broadband Radiation Generation

The purpose of this section is to present an outline of the analysis that demonstrates UB radiation generation from a single pulse or from the beating of two laser pulses with differing frequencies (laser beat waves). Ultra broadband radiation can be generated in a nonlinear optical medium with pico-second laser pulses. In the past, the single pulse conversion efficiency and bandwidth have been impressive, but average power has been limited to relatively modest values.[2,3] Recently, a new method has been proposed for generating high average power UB radiation.[5] In this method, UB radiation is generated by beating two laser beams with slightly different frequencies in a nonlinear medium.[5] The conversion efficiency for this process can be shown to be relatively high, and the bandwidth of the radiation can be on the order of 100%. Especially in the 3-8 μm wavelength region, where there is a lack of available laser sources, the UB radiation can provide the necessary illumination required for active remote sensing. The source size of the UB radiation is extremely small, which allows for beaming the radiation extended distances, beyond 3 km.

Lasers with optical (~ 0.5 μm) and near-IR (~ 1 μm) wavelengths can be used to generate UB from ~ 0.4 μm to ~ 3 μm. To reach longer wavelength regions, CO_2 lasers may be used. These lasers are line-tunable in the 9-11 μm range. If two closely-spaced CO_2 laser lines are selected, the beating of these lines in an appropriate nonlinear medium such as gallium arsenide

can lead to substantial spectral broadening, thus covering the mid and far IR regions of the spectrum. In principle, the conversion efficiency and bandwidth can be optimized by selecting the appropriate nonlinear medium and adjusting the beat frequency, power, and spot size of the laser.

A. UB Generation Using a Short Laser Pulse

The longitudinal gradients in the intensity of a single laser pulse can lead to frequency up-shifting and broadening via self-phase modulation. Consider the nonlinear index of refraction resulting from the $\chi^{(3)}$ (third-order susceptibility) nonlinearity, $n \equiv n_0 + n_2 I$, where n_0 is the linear index, I is the laser intensity, n_2 is the nonlinear index, $n_2 I = 2\pi\chi^{(3)}E^2/n_0$, and E is the electric field of the laser pulse. The change in phase $\delta\phi$ for a laser field $E \sim \exp i(k_0 z - \omega_0 t + \delta\phi)$ which propagates into a nonlinear medium is given by $\delta\phi = (\omega_0/c)\int dz n_2 I \equiv (\omega_0/c) n_2 I z$, where ω_0 and k_0 are the nominal frequency and wave number of the laser field and z is the axial propagation distance. The change in frequency is given by $\delta\omega = -\partial\delta\phi/\partial t$. Hence, as the laser pulse propagates, new frequencies are generated [2,6,7]

$$\delta\omega \equiv -z(\omega_0 / c) n_2 \partial I / \partial t. \qquad (1)$$

In particular, at the front of the pulse $\partial I/\partial t > 0$ and the local frequency is down-shifted, whereas at the back of the pulse $\partial I/\partial t < 0$ and the local frequency is up-shifted. The above simple estimate is valid for small frequency shifts $|\delta\omega| << \omega_0$. For ultra-short pulses, the intensity gradients can be very large which results in large frequency shifts and the generation of a supercontinuum.

Spectral broadening has been observed experimentally with ultrashort laser pulses, i.e., pulse durations on the order $\tau \leq 1$ ps. Using femtosecond laser pulses with a wavelength $\lambda_0 \sim 1$ μm, a spectral broadening of 20,000 cm^{-1} is readily achievable in a condensed medium.[2] Short

pulses are necessary in order to achieve large intensity gradients, $\partial I/\partial t \sim I/\tau$. The use of ultrashort pulses has its limitations: (i) the supercontinuum generated is also short pulsed (≤ 1 ps) and, perhaps more importantly, (ii) the repetition rate and hence the average power of the generated radiation is low, due to the low repetition rate and low average power of the short pulse laser.

B. UB Generation Using Two Beating Lasers

Supercontinuum generation, in principle, can be achieved using the beat wave produced by the interaction of two long pulse laser beams of two different frequencies, ω_1 and ω_2, within a nonlinear medium. Consider, for example, two linearly polarized lasers with electric fields given by

$$\underset{\sim}{E}_1 = \hat{E}_1 \cos(k_1 z - \omega_1 t)\hat{e}_x, \tag{2a}$$

$$\underset{\sim}{E}_2 = \hat{E}_2 \cos(k_2 z - \omega_2 t)\hat{e}_x, \tag{2b}$$

where $k_{1,2}$ are the wave numbers and $\hat{e}_x$ is the unit vector. Within the nonlinear medium, these two fields will interact to produce a beat wave via the $\chi^{(3)}E^2$ term in the nonlinear polarization field. Assuming equal amplitudes, $\hat{E}_1 = \hat{E}_2 = A_0 / 2$, we have

$$\underset{\sim}{E} = \underset{\sim}{E}_1 + \underset{\sim}{E}_2 = A_0 \cos(k_0 z - \omega_0 t)\cos\left(\frac{\Delta k}{2} z - \frac{\Delta\omega}{2} t\right)\hat{e}_x, \tag{3}$$

where $\omega_{1,2} = \omega_0 \pm \Delta\omega/2$, $k_{1,2} = k_0 \pm \Delta k/2$, and $\omega_1 - \omega_2 = \Delta\omega$. Hence, $|E_1 + E_2|^2$ represents a beat wave, i.e., the intensity envelope I of the two laser fields is modulated at the beat frequency $\Delta\omega \equiv \omega_1 - \omega_2$,

$$I \sim \left\langle \left| E_1 + E_2 \right|^2 \right\rangle = \left(A_0^2 / 4 \right)[1 + \cos(\Delta k z - \Delta\omega t)], \tag{4}$$

where < > represents a time average over the fast frequency ω_0. In effect, the longitudinal intensity profile resembles a train of short pulses of duration $\tau \sim 1/\Delta\omega$ and results in large gradients in the intensity $\partial I/\partial t \sim \Delta\omega I$. Likewise, the induced frequency, as given by Eq. (1),

$$\delta\omega / \omega_0 \cong z(\Delta\omega / c) n_2 I, \tag{5}$$

can be large. As an example, consider two laser beams operating on two CO_2 lines, $\lambda_1 = 10.5$ μm and $\lambda_1 = 10.6$ μm. Hence, $\Delta\omega = 2\pi c(1/\lambda_1 - 1/\lambda_2) = 1.7 \times 10^{12}$ sec^{-1} and $\tau = 1/\Delta\omega = 590$ fs. Since the two laser beams are long pulse, the resulting radiation can be long pulse with relatively high average power.

C. Fully Nonlinear and Dispersive Model of Spectral Broadening

The two-dimensional nonlinear evolution of a short laser pulse in a nonlinear medium is described by the wave equation

$$\left(\frac{\partial^2}{\partial z^2} - \frac{1}{c^2}\frac{\partial^2}{\partial t^2} - k_\perp^2 \right) \underset{\sim}{E} = \frac{4\pi}{c^2}\frac{\partial^2}{\partial t^2} \underset{\sim}{P}_p, \tag{6}$$

where $k_\perp = 2/r_0$ is the transverse wave number, r_0 is the spot size, and $\underset{\sim}{P}_p$ is the complete polarization field. It is convenient to use the notation $\underset{\sim}{E} = A \exp\left[i(k_0 z - \omega_0 t)\right] \hat{e}_x$, where A is the slowly varying electric field amplitude. In the following, $k_\perp = 0$ will be assumed.

Injecting two laser beams of slightly different frequencies into the nonlinear medium can provide spectral broadening together with high average power. The initial optical field is taken to be

$$\underset{\sim}{E}(z=0) = (A_0/2)\cos\left((k_0 - \Delta k/2)z - (\omega_0 - \Delta\omega/2)t\right)\hat{e}_x$$

$$+ (A_0/2)\cos\left((k_0 + \Delta k/2)z - (\omega_0 + \Delta\omega/2)t\right)\hat{e}_x$$

$$= A_0 \cos(\Delta\omega\tau/2)\cos(\omega_0\tau)\hat{e}_x, \qquad (7)$$

where A_0 is the real and constant amplitude, $k_0 = n_0\omega_0/c = \omega_0/v_g$, $\Delta k = \Delta\omega/v_g$ is the difference in wave numbers of the two lasers, $\Delta\omega$ is the frequency difference, $\tau = t - z/v_g$, v_g is the linear group velocity. The power associated with the optical field is $P = cr_0^2 n_0 |A|^2 / 16$. It is convenient to introduce the complex field amplitude $\tilde{P}^{1/2} = \left(cr_0^2 n_0 / 16P_N\right)^{1/2} A$, such that $\left|\tilde{P}^{1/2}\right|^2 = P/P_N$ is the normalized power, where $P_N = 2\pi c^2/(\omega_0^2 n_0 n_2)$ is the critical power for nonlinear self-focusing. Defining $\tilde{z} = z/L_0$, $L_0 = n_0 Z_R/2$, and $Z_R = \omega_0 r_0^2/2c$, the wave equation can be solved for the complex amplitude and cast into the following normalized form:

$$\partial\tilde{P}^{1/2}/\partial\tilde{z} = i\left(1 + i(\omega_0\tau_0)^{-1}\partial/\partial\tilde{\tau}\right)\left(|\tilde{P}|\tilde{P}^{1/2}\right)$$

$$- i(1/2)R_2\partial^2\tilde{P}^{1/2}/\partial\tilde{\tau}^2 + (1/6)R_3\partial^3\tilde{P}^{1/2}/\partial\tilde{\tau}^3. \qquad (8)$$

Here $\tilde{\tau} = \tau/\tau_0 = (t - z/v_g)/\tau_0$ is the normalized time in a frame moving with the group velocity, τ_0 is a characteristic pulse time or period, $R_2 = L_0/L_{D2}$ and $R_3 = L_0/L_{D3}$. The first and second order dispersion distances are, respectively,

$$L_{D2} = \tau_0^2/H_2, \qquad (9a)$$

$$L_{D3} = \tau_0^3/H_3, \qquad (9b)$$

where in the $k_\perp = 0$ limit, the quantities H_2 and H_3 are the usual group velocity dispersion (GVD) coefficients β_2 and β_3 [3]. For $P = P_N$, the distance L_0 is the same as the "nonlinear distance" described in Ref. 3. The initial value of $\tilde{P}^{1/2}$ at $\tilde{z} = 0$ is

$$\tilde{P}^{1/2}(z=0,\tau) = (P_0(0,\tau)/P_N)^{1/2}\cos(\Delta\omega\tau/2)\,, \tag{10}$$

where $P_0(0,\tau)$ is the initial axial profile of the power.

In the absence of dispersion, $R_2 = R_3 = 0$, the reduced wave equation in Eq. (8) becomes

$$\frac{\partial\tilde{P}^{1/2}}{\partial\tilde{z}} \cong i\left(1 + i\omega_0^{-1}\frac{\partial}{\partial\tau}\right)\left(|\tilde{P}|\tilde{P}^{1/2}\right). \tag{11}$$

The evolution of the amplitude $\tilde{P}_0^{1/2}$ and phase ϕ of $\tilde{P}^{1/2}$ is given by

$$\frac{\partial\tilde{P}_0^{1/2}}{\partial\tilde{z}} = -\omega_0^{-1}\frac{\partial}{\partial\tau}\tilde{P}_0^{3/2}, \tag{12a}$$

$$\frac{\partial\varphi}{\partial\tilde{z}} = \left(1 - \omega_0^{-1}\partial\varphi/\partial\tau\right)\tilde{P}_0^{1/2}, \tag{12b}$$

where $\tilde{P}^{1/2} = \tilde{P}_0^{1/2}\exp(i\phi)$ and the initial conditions (at $z = 0$) for $\tilde{P}_0^{1/2}$ are given by Eq. (10).

Equations (8) can be used to describe self-phase modulation, continuum generation, and soliton formation, including the effects of group velocity dispersion and finite $\chi^{(3)}$. The standard theory [2] of self-phase modulation and continuum generation for ultrashort pulses neglects the effects of group velocity dispersion, i.e., the terms proportional to R_2 and R_3 are neglected. In standard soliton theory [3,8], the first term on the right of Eq. (8) is neglected. Equation (8) allows continuum generation and solitons to be studied self-consistently including these effects. In particular, it can be used to study self-phase modulation, continuum generation, and soliton formation for a beat wave produced by two lasers of different frequencies, as described by Eqs.

(2a) and (2b). Numerical solutions to Eq. (8) are described in the next section. These results show that dispersion effects can significantly modify the spectrum even when the dispersive terms R_2 and R_3 are small.

D. Lowest Order Solution in the Absence of Dispersion

Approximate solutions to Eq. (12), for small variations in the amplitude and frequency, are

$$P \equiv P_0 \cos^2(\Delta\omega\tau/2)\left(1+\frac{3}{2}\frac{\Delta\omega}{\omega_0}\frac{P_0}{P_N}\frac{z}{L_0}\sin(\Delta\omega\tau)\right), \tag{13a}$$

$$\omega \equiv \omega_0\left(1+\frac{1}{2}\frac{\Delta\omega}{\omega_0}\frac{P_0}{P_N}\frac{z}{L_0}\sin(\Delta\omega\tau)\right), \tag{13b}$$

where $\Delta\omega = \omega_0\Delta\lambda/\lambda_0$ is the initial frequency difference, and $\Delta\lambda$ is the wavelength difference.

III. Numerical Results for UB Radiation Generation

Equation (8) has been solved numerically using the split-step Fourier method, a pseudospectral numerical technique which has been widely-used in modeling nonlinear effects in fiber optics.[3,9] The initial amplitude $\tilde{P}^{1/2}(z = 0, \tau)$ is specified, and the complex amplitude $\tilde{P}^{1/2}$ is calculated using a step size Δz which is small compared with L_0. Since a fast Fourier transform (FFT) is used, the number of grid points in τ must be a power of two, and the waveform must go to zero near the boundaries to avoid aliasing effects. For the two laser beat-wave case, it is convenient to chose $\tau_0 = \Delta\omega^{-1}$ and specify $P_0 = P_N$. In addition, one must specify the normalized input parameters $\Delta\omega/\omega_0$, L_{D2}/L_0, and L_{D3}/L_0.

Ultra broadband radiation is traditionally produced by using a single short pulse or a train of isolated pulses, and numerical solutions to an equivalent form of Eq. (8) for such pulses are extensively described in Ref. 3. Figure 2 plots the normalized power $\tilde{P}(\tau)$ at locations $z/L_0 = 0$ and 17 for a single pulse with $\tilde{P}^{1/2}(z = 0, \tau) = \exp(-\tau^2/2\tau_o^2)$ and $\omega_0\tau_0 = 45$. This Gaussian pulse case neglects dispersion. One can show analytically [3] that in the limit of zero dispersion, the steepening on the back side of the pulse should reach an infinite slope at $z/L_0 = 0.39\omega_0\tau_0$, a result which is consistent with the numerical solution in Fig. 2. This steepening causes substantial broadening in the power spectrum $S(\omega)$, which is calculated by taking $S(\omega) = \tilde{P}_k^{1/2}(\omega)(\tilde{P}_k^{1/2}(\omega))^*$ where $\tilde{P}_k^{1/2}(\omega)$ is the Fourier transform of $\tilde{P}^{1/2}(\tau)$, and $(\tilde{P}_k^{1/2}(\omega))^*$ is its complex conjugate. Figure 3 plots $S(\omega)$ at $z/L_0 = 17$ and shows the frequency spread is comparable to ω_0, indicating the generation of ultra broadband radiation. The oscillations in the spectrum are consistent with the modulation commonly observed in many experiments.[2,10]

Qualitatively similar spectra can be produced for the laser beat-wave technique described in Section II. Figure 4 shows the power spectrum $S(\omega)$ at $z/L_0 = 80$ for a case with $\Delta\omega/\omega_0 = 0.01$ and a very small amount of dispersion ($R_2 = 3\text{x}10^{-4}$). The power spectrum consists of discrete lines separated by $\Delta\omega$ and shows significant spectral broadening, especially in the anti-Stokes direction ($\omega > \omega_0$). Even this small amount of dispersion is sufficient to change the numerical solution significantly. For $R_2 = 0$, the model gives an optical shock and substantial spectral broadening at $z/L_0 = 45$, and the numerical method breaks down shortly after that point.

Although most analyses of ultra broadband radiation neglect dispersion, it is clear that dispersion plays a major role when parameters corresponding to most real materials and

experiments are used. For a single Gaussian pulse with a small but nonzero R_2, the pulse flattens and spreads after propagating in z over a distance which is typically only 10-20% of the characteristic dispersion distance L_{D2}.[3] This is accompanied by a strong steepening at the edge of the pulse and the generation of high frequency edge oscillations.[3] An analogous process is predicted to occur in the beating laser case, except that the spreading of the waveform on the $\Delta\omega^{-1}$ time scale is clearly constrained by the next half-oscillation in the waveform.

Figure 5 plots $\tilde{P}(\tau)$ at $z/L_0 = 0$, 10, 20, and 30 for a beating laser case with $\Delta\omega/\omega_0 = 0.01$, $R_2 = 3.8\text{x}10^{-3}$, and $R_3 = 4\text{x}10^{-4}$. These parameters are appropriate for the proof-of-principle experiment described in Section V, operating at $\tilde{P}_0 = 1$ in a fused silica optical fiber with a peak intensity of $2\text{x}10^{11}$ W/cm^2. The figure shows three half-oscillations of the beating waveform. As the laser propagates, fast oscillations eventually form at the boundaries between successive half-oscillations. Figure 6 plots the power spectrum $S(\omega)$ at $z/L_0 = 30$. The spectrum is relatively flat except for the harmonic structure at $\Delta\omega$ and extends to about 15% of the central frequency ω_0 in both the Stokes and anti-Stokes directions. This spread is typical of many single pulse experiments in optical fibers.[2,3,10]

Larger spreads in the power spectrum can in principle be produced by optimizing the frequency mismatch $\Delta\omega$, increasing the laser intensity, propagating further into the fiber, or choosing a material with a lower dispersion parameter at 1.06 μm. Higher laser intensities can lead to breakdown and permanent damage to the material, while propagating too far into the material produces little additional spreading and tends to give a nosier spectrum. The choice of the optimal $\Delta\omega$ involves a tradeoff between the propagation distance required for the desired frequency spread and dispersion effects. Equation (13a) shows that reducing $\Delta\omega/\omega_0$ can

substantially reduce undesirable dispersion effects, but Eq. (13b) shows that it increases the distance z required to achieve a given spread in ω/ω_0.

The numerical model has also been used to evaluate potential ultra broadband sources using two closely-spaced lines from a CO_2 laser and gallium arsenide as the nonlinear medium. Again dispersion plays a major role in determining the spectrum. Gallium arsenide exhibits anomalous dispersion ($\beta_2 < 0$) in this regime, which results in cusp-like spikes on the waveform and significant spectral broadening after only a few Rayleigh lengths of propagation. Preliminary results suggest that in the 9 μm regime, a 2% mismatch in the wavelengths may produce significant radiation down to 6 μm. This case, which is shown in Fig. 7, used $L_0/L_{D2} = 0.2$ and $L_0/L_{D3} = 0.027$, which corresponds to $P = P_N$ and an intensity of 10^{10} W/cm^2. Spectral broadening can be overwhelmed by dispersion when the dispersion length is comparable to the Rayleigh length, so relatively small changes in parameters could modify the spectrum considerably in this parameter regime. Ultra broadband radiation using a single pulse CO_2 laser was first reported by Corkum, et al.[11]

IV. Three Wavelength DIAL

The use of DIAL for remote sensing of chemical species in the atmosphere is a well known technique that can detect and identify a wide range of molecular constituents. However, DIAL is presently operated with two distinct laser wavelengths when the absorption coefficients of the chemical species are known as a function of wavelength. When using only two frequencies, one needs to know the target reflectivity and the extinction coefficient of the atmosphere (which are not typically known) at these wavelengths to obtain accurate measurements.

Knowledge of the dependence of the reflectivity and extinction coefficient on wavelength is not necessary if three or more frequencies are used. If a third frequency is used, which is symmetrically located on either side of the absorption peak, as shown in Fig. 8, it can be shown that the pollutant density can be determined independently of the reflectivity and extinction coefficient of the background. We are assuming here that the dependence of the background reflectivity and extinction coefficient have a weak linear dependence on wavelength. The pollutant density is then simply a function of the received power at the three wavelengths. Using three specific wavelengths can therefore yield far more accurate values for the pollutant density. The UB transmitting signal can serve as a three wavelength DIAL system over multiple absorption bands. Each pollutant will absorb its characteristic radiation, which can be detected, identified, and analyzed, yielding both the range and concentration.

Using the LIDAR equation [1] it can be shown that using three wavelengths, λ_0, λ_1, and λ_2, the minimum density of the pollutant N is given by

$$N = \frac{\ell n\left(\sqrt{P_r(\lambda_1)P_r(\lambda_2)} / P_r(\lambda_0)\right)}{2R\left(\sigma(\lambda_0) - \sigma(\lambda_1)\right)}, \qquad (14)$$

where $P_r(\lambda)$ is the power received at the detector at wavelength λ, R is the range, and $\sigma(\lambda)$ denotes the absorption cross section at wavelength λ. As an illustration consider a pollutant at a range of R ~ 1 km and a signal strength $P_r(\lambda_{1,2})/P_r(\lambda_0) \approx 2$. The sensitivity of a three wavelength DIAL system is $N/N_0 = 1.3 \times 10^{-8}$ for the pollutant SO_2 having a cross section of $\sigma(\lambda = 0.8 - 1\ \mu m) \approx 10^{-17}\ cm^2$, where N_0 is the ambient air density.

V. Experimental Approach for Ultra Broadband Radiation Generation

The generation of UB radiation will be carried out at the Naval Research Laboratory (NRL) using available laser facilities. Single laser pulses with sub-picosecond pulse durations from the Table Top Terawatt laser have been used to demonstrate the generation of ultra broadband radiation. High average power UB radiation in nonlinear media can be generated with long pulse lasers modulated at subpicosecond periods. This can be achieved in two possible arrangements. The first is to inject two laser pulses with slightly different frequencies in a nonlinear medium, and the second is to inject a single laser pulse into a Raman cell in order to generate a second frequency within the pulse prior to injection into the nonlinear medium.

Two mode-locked lasers at NRL are available for this experiment. One laser is a Nd:YAG laser with wavelength equal to 1.064 μm, energy of 300 mJ per pulse and pulse duration of 300 psec. Another laser is a Nd:Glass laser with wavelength equal to 1.053 μm and similar pulse energy and duration. These two lasers can be synchronized with each other by using the same RF driver for their mode-lockers. Exact synchronization will be achieved with optical delay lines. The laser beams are then adjusted to have the same divergence, so that, when focused they will overlap at the same axial position. The lasers will also be aligned to overlap transversely at the focal plane. The angular separation of the two lasers will also be minimized to obtain the maximum overlap. The wavelength difference of 10 nm between the two lasers will create a modulation period of 300 fsec. The pulse energy of the two lasers will be adjusted to be approximately the same to ensure large amplitude modulation in the beat wave created.

Alternatively, a single laser may be used to generate the modulated pulse. A Raman cell containing a suitable nonlinear medium can be used to generate a second wavelength utilizing the Raman interaction. Different nonlinear media can impart different Raman shifts from the

fundamental for the second laser frequency. For example, carbon disulfide can produce a Raman shift of ~80 nm for a fundamental wavelength of 1.064 μm, while carbon tetrachloride will generate a shift of ~56 nm. These wavelength differences between the two laser frequencies will generate modulation periods of 38 fsec and 54 fsec respectively. The advantage of using the Raman cell to generate the second laser frequency is that the two laser lines are naturally synchronized and aligned. However, it is more difficult to adjust the relative energies in the two laser lines by controlling the conversion efficiency. One could split the two laser lines and attenuate one of them to obtain equal proportion of energy in each line. However, the necessity of recombining the two lasers requires delicate alignment similar to using two different lasers.

The modulated laser beam will then pass through a suitable nonlinear medium for generating the UB radiation. The sub-picosecond structures in the laser pulse will generate the UB radiation through the mechanism of self-phase modulation. Experiments will be performed using various media with high nonlinear index of refraction including liquids and solid state materials. Liquids have the advantage of self-healing, which is desirable for laser intensities approaching the laser breakdown thresholds. Solid material will be used at lower laser intensities. Interaction distances long compared to the diffraction length are desirable, and, hence, optical fibers are natural candidates for the nonlinear medium. Suitable optical fibers will be used to study the UB radiation generation by modulated long laser pulses.

VI. Summary

Ultra broadband (UB) radiation is a promising source for active remote sensing. It can be readily produced by propagating intense, short laser pulses in appropriate solids or liquids. In this

report, we assess the feasibility of using two long pulse, mode-locked lasers with a small separation $\Delta\omega$ in frequency to generate UB radiation. Such a system may be less expensive and more compact than single rep-rated short pulse lasers while operating at substantially higher average powers. The theory of UB generation with laser beat waves is presented, including the effects of self-phase modulation, nonlinear steepening, and both first and second order dispersion. Numerical solutions to the model equation show parameters regimes where UB generation may be expected. Dispersion plays a major role in the spectral broadening, so both laser and material parameters must be carefully chosen. As expected, the behavior for laser beat waves is similar in many cases to that for a single pulse with the pulse width replaced by the beat wave period, $\Delta\omega^{-1}$.

One application of the UB source is for multi-wavelength DIAL to determine concentrations of hazardous pollutants. Conventional DIAL systems use only two wave-lengths, but the addition of a third wavelength can eliminate the requirement that the reflectivity and extinction coefficients be known.

Finally, a proof-of-principle experiment for UB generation using laser beat waves is outlined. The experiment would use two existing mode-locked lasers at NRL operating at 1.064 μm and 1.053 μm, with an alternative approach using a single laser and a Raman cell to shift a portion of the radiation for the second wavelength. Initial experiments will be carried out using liquids or optical fibers as the nonlinear media.

Acknowledgments:

The authors acknowledge useful discussions with J. Krall, G. Joyce, K. Krushelnick, G. Ganguli, J. Grun, and R. Burris. This work was supported by the SERDP Compliance Program under Research Project # R3715SERDP and the Office of Naval Research.

References

[1] *Laser Remote Chemical Analysis*, edited by R. M. Measures (Wiley, New York, 1988).

[2] *The Supercontinuum Laser Source*, edited by R. R. Alfano (Springer, New York, 1989).

[3] G. P. Agrawal, *Nonlinear Fiber Optics* (Academic, San Diego, 1995).

[4] R. R. Alfano and S. L. Shapiro, Phys. Rev. Lett. **24**, 584 (1970); R. R. Alfano and S. L. Shapiro, Phys. Rev. Lett. **24**, 592 (1970).

[5] S. Sprangle, E. Esarey, and R. Hubbard, to be submitted to Phys. Rev. E (1996).

[6] R. W. Boyd, *Nonlinear Optics,* (Academic Press, New York, 1992).

[7] Y. R. Shen, *The Principles of Nonlinear Optics* (Wiley, New York, 1984).

[8] *Optical Solitons - Theory and Experiment,* Cambridge Studies in Modern Optics **10**, Edited by J. R. Taylor (Cambridge University Press, Cambridge, 1992).

[9] R. H. Hardin and F.D. Tappert, SIAM Rev. Chronicle **15**, 423 (1973).

[10] P. L. Baldeck, P. P. Ho, and R. R. Alfano, Rev. Phys. Appl. **22**, 1877 (1987).

[11] P. Corkum, P. Ho, and R. Alfano, Opt. Lett. **10**, 624 (1995).

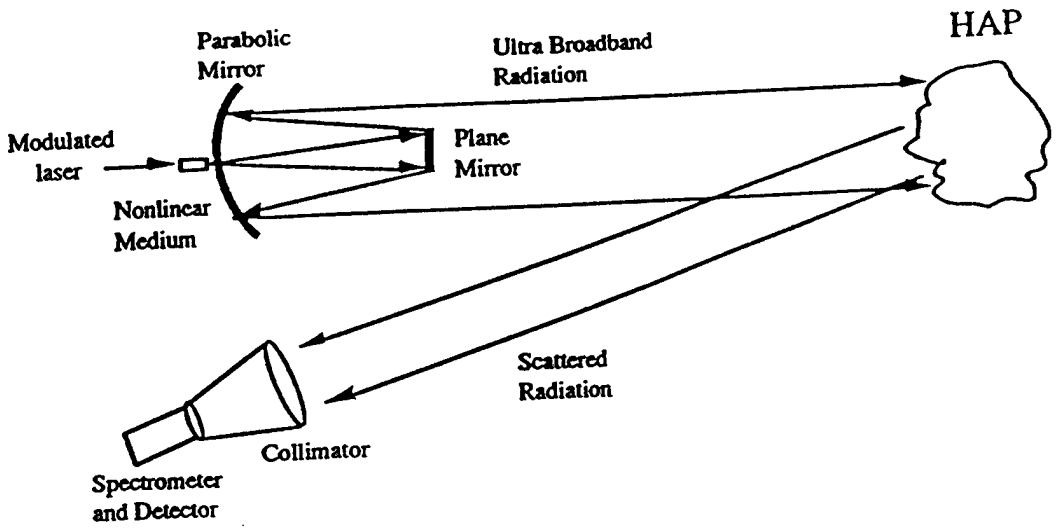

Fig. 1. Schematic of active remote sensing using ultra broadband radiation.

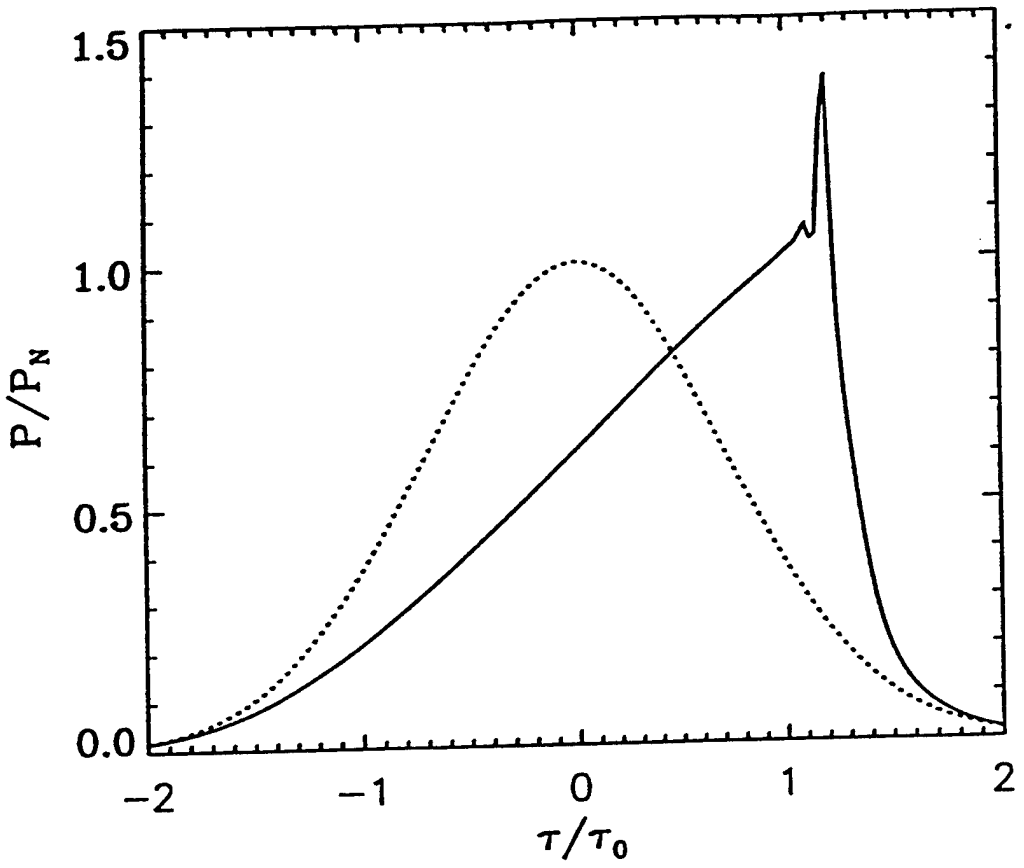

Fig. 2. Plot of the normalized power $\tilde{P}(\tau) = P(\tau)/P_N$ at $z/L_0 = 0$ (dotted line) and 17 (solid) for a single pulse with a Gaussian shape $\tilde{P}^{1/2}(z = 0, \tau) = \exp(-\tau^2/2\tau_o^2)$ and $\omega_0\tau_0 = 45$. This case neglects dispersion and is calculated numerically from Eq. (12).

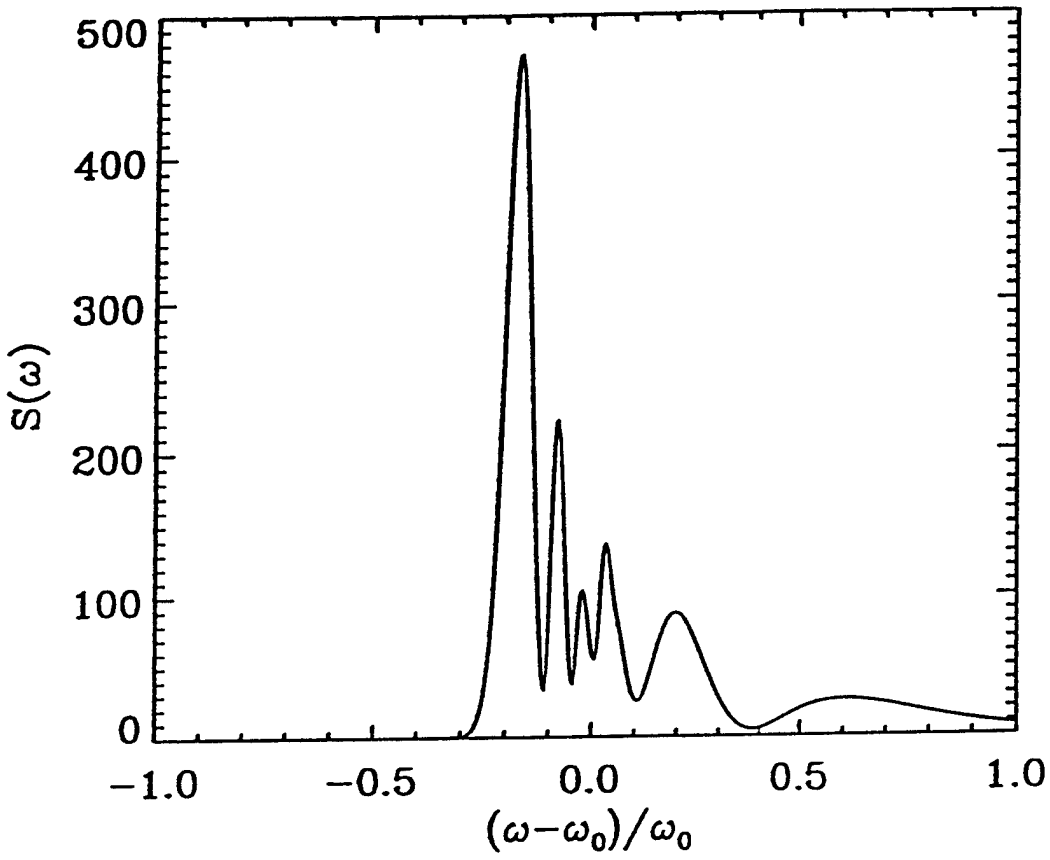

Fig. 3. Plot of the power spectrum $S(\omega)$ in arbitrary units at $z/L_0 = 17$ for the Gaussian pulse case shown in Fig. 2. The frequency spread is comparable with the initial laser frequency.

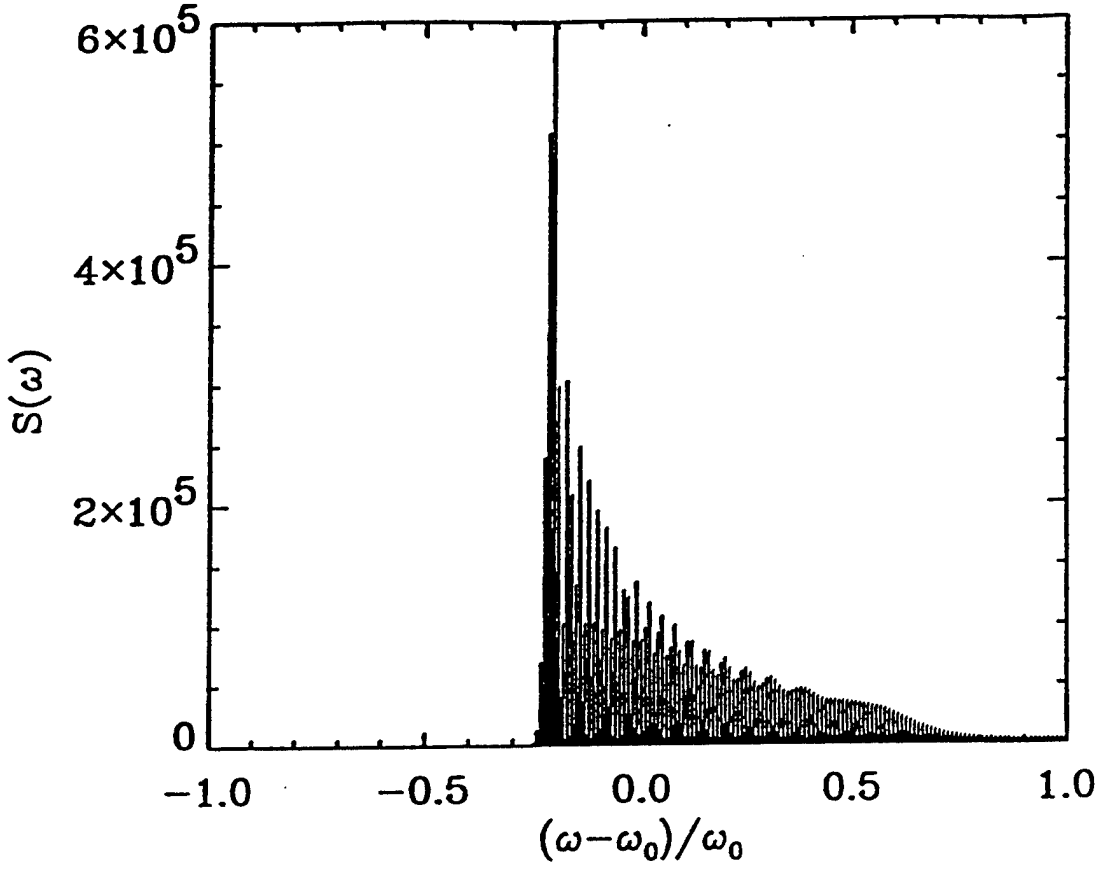

Fig. 4. Model calculation of the power spectrum (arbitrary units) for a laser beat wave example with frequency separation $\Delta\omega/\omega_0 = 0.01$ and the dispersion parameter $R_2 = 0.0003$. Spectrum is similar to the single pulse case but shows discrete lines separated by $\Delta\omega$.

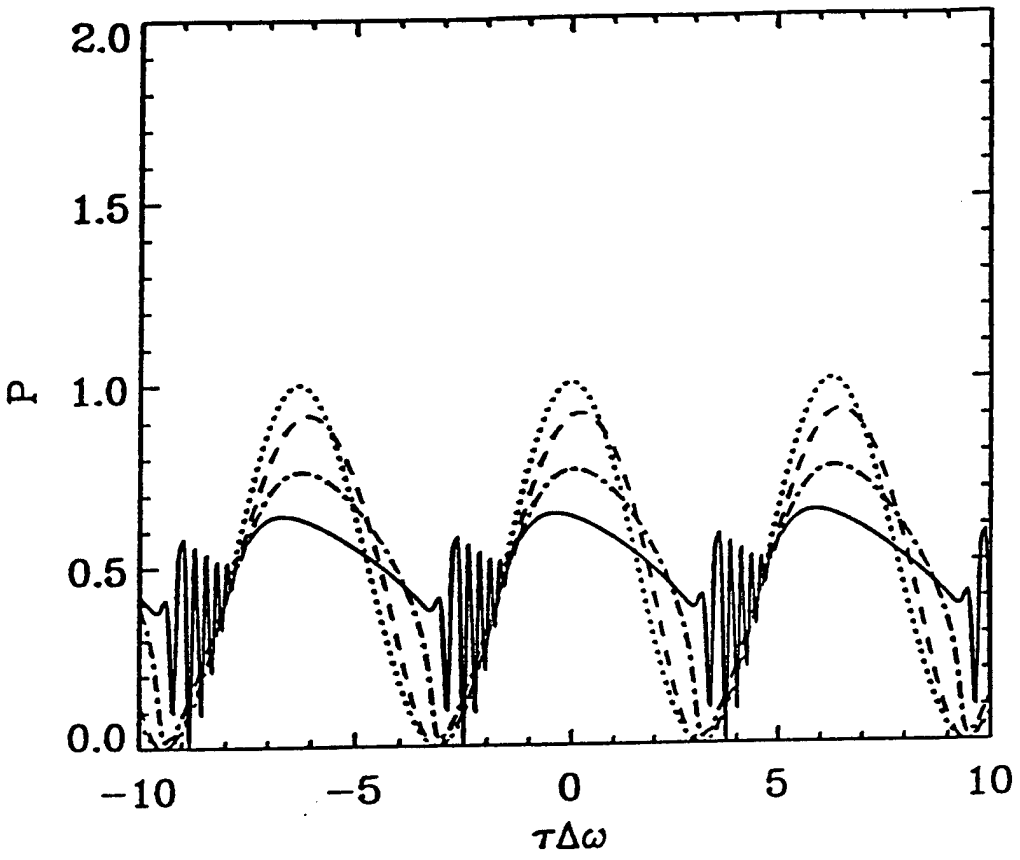

Fig. 5. Plot of the normalized power $\tilde{P}(\tau)$ for a laser beat wave case with $\Delta\omega/\omega_0 = 0.01$, $R_2 = 0.0038$, and $R_3 = 4\text{x}10^{-4}$. Individual curves are at $z/L_0 = 0$ (solid curve), 10 (dash), 20 (dot-dash), and 30 (solid).

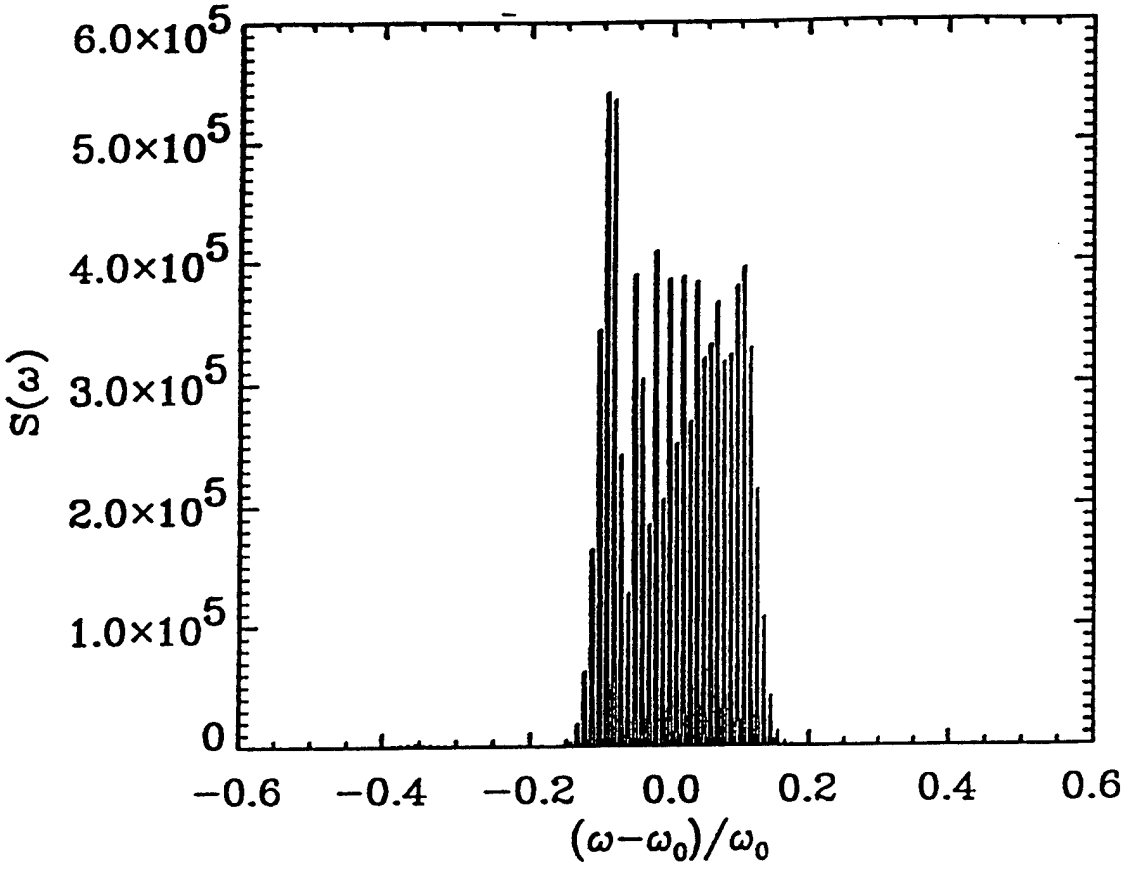

Fig. 6. Plot of the calculated power spectrum $S(\omega)$ in arbitrary units at $z/L_0 = 30$ for the laser beat-wave example shown in Fig. 5.

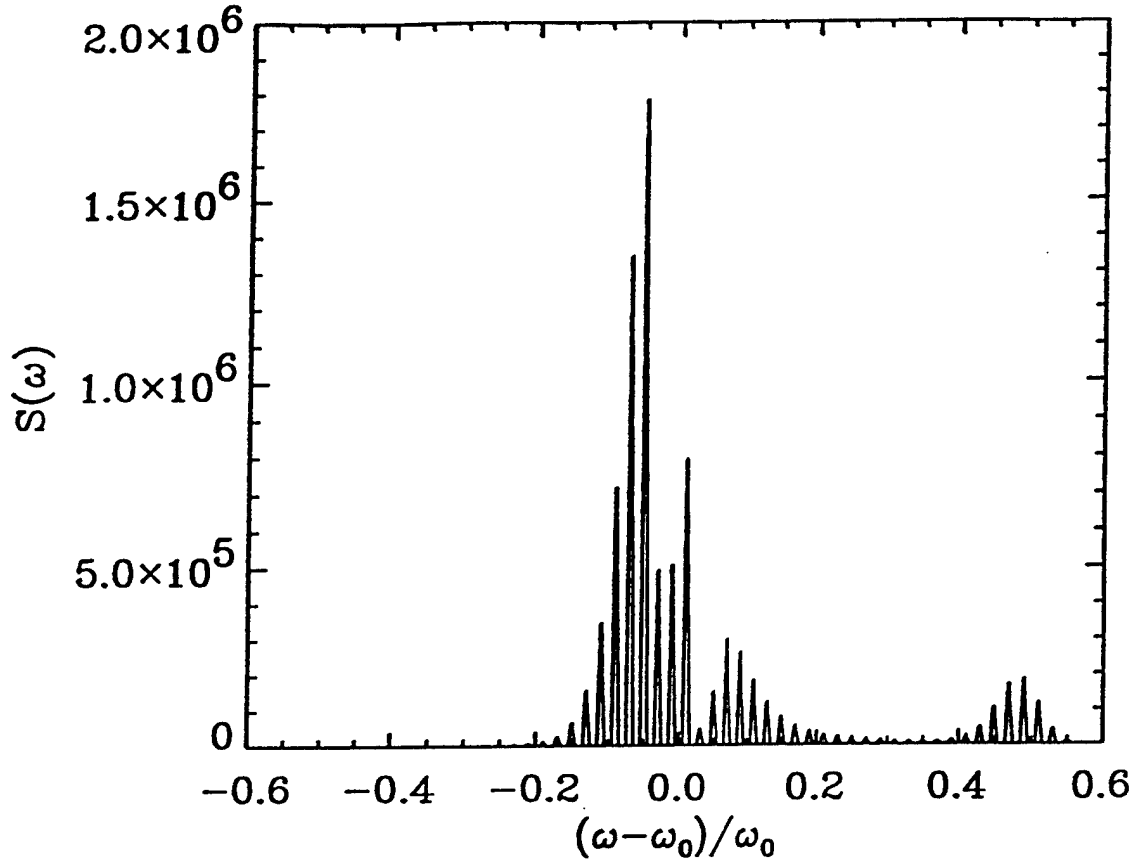

Fig. 7. Plot of the calculated power spectrum $S(\omega)$ at $z/L_0 = 4$ for a case with $\Delta\omega/\omega_0 = 0.02$, $R_2 = -0.20$, and $R_3 = 0.027$. The parameters for this anomalous dispersion case ($R_2 < 0$) are appropriate for using two lines from a CO_2 laser as the source and gallium arsenide as the nonlinear medium

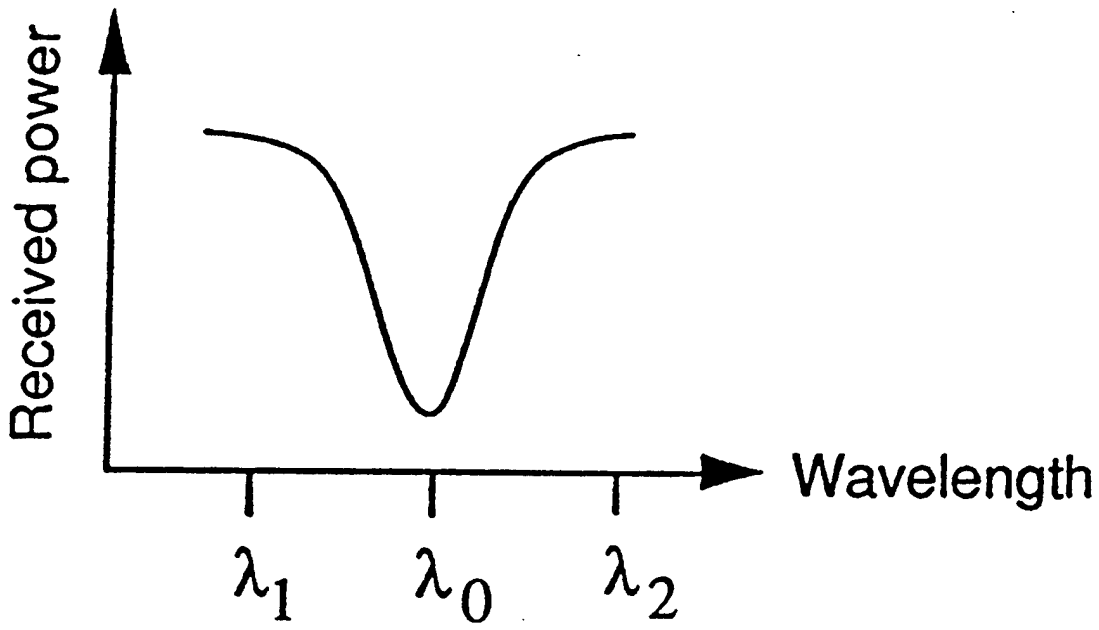

Fig. 8. Locations of three wavelengths around an absorption peak. The differences in received power are used in a three wavelength DIAL scheme to calculate concentrations of the trace specie.